Inhibition of the pitting corrosion of 304 stainless steel in 0.5 M hydrochloric acid solution by heptamolybdate ions

Y. AIT ALBRIMI[1], A. AIT ADDI[1], J. DOUCH[1], R.M. SOUTO[2], M. HAMDANI[1]

[1]*Laboratoire de Chimie Physique, Faculté des Sciences, Université Ibn Zohr, B.P. 8106 Cité Dakhla, Agadir, Maroc.*

[2]*Department of Chemistry, University of La Laguna, P.O. Box 456, E-38200 La Laguna (Tenerife, Canary Islands), Spain.*

Abstract:

The corrosion inhibition effect of heptamolybdate ions on 304 stainless steel in 0.5 M hydrochloric acid solution at 298 K was investigated using gravimetric, electrochemical and optical microscopy methods. Increasing inhibitor concentration led to significant reduction in the corrosion rate of stainless steel, withinhibitor efficiency values above 90%. The adsorption of the inhibitor onto the steel surface is described using the Langmuir adsorption isotherm. The value of the free energy of adsorption determined at 298 K ($\Delta G°$ = -31.1 kJ mol^{-1}) characterizes the adsorption process of heptamolybdate ions on the surface of the metal.

Keywords: 304 Stainless steel; Pitting; Corrosion inhibition; Heptamolybdate ions; Hydrochloric acid.

1. Introduction

Austenitic stainless steels (SS) are widely used due to their high corrosion resistance and strength. The high corrosion resistance of these materials arises from the formation of a passive layer on their surface. This is usually a duplex film constituted by an outer iron and chromium oxy-hydroxide layer and water containing compounds formed at the metal/solution interface, and an inner compact layer formed by chromium oxide [1]. The corrosion resistance of passivated stainless steel is often limited by its susceptibility to local breakdown and pit nucleation. Aggressive ions such as chloride produce local breakdown of the protective layers formed at the steel-solution interface (either passive oxide layers or inhibitor-containing films), causing pitting corrosion [2], which is one of the most dangerous forms of localized corrosion [3]. Chloride ions promote localized breakdown of the protective passive layer, leading to the formation of corrosion pits [4,5]. Passivity breakdown occurs at small areas of the steel in contact with the aggressive environment while most of it remains passive. The formation of corrosion pits occurs though nucleation and two distinguishable propagation stages, initially metastable growth, eventually followed by stable growth [2,6,7]. Hydrochloric acid, briny water, sea water and misty fog occurring near the sea, are the main sources of chloride ions.

An efficient method to prevent the corrosion of equipments from steel, and consequently extend their life, is the use of corrosion inhibitors. Organic molecules containing sulphur, nitrogen or oxygen atoms produce inhibitory effects towards the corrosion of steel in acidic media. They reduce the rates of either the anodic or the cathodic reactions, resulting in the reduction of the overall corrosion rate of the material. Though a large number of corrosion inhibitors have become available throughout the years, the scientific literature shows significant research activities directed to find cheaper, non-toxic, environmentally-friendly inhibitors that may be ecologically acceptable from a safety standpoint [8,9]. Current trends and novel approaches in the field of inhibitor technology for corrosion protection have been described in a recent review [10]. Inhibitors may afford corrosion protection by covering the surface of the steel and blocking reactive sites through the formation of insoluble compounds at them. They may also alter the pH or the ionic composition at the interface, and contribute to the repassivation (by oxide film formation) of a bare steel surface originating from the breakdown of the oxide film [11].

Molybdate ion, MoO_4^{2-}, with low toxicity and good environmental acceptability, can be regarded the most versatile inhibitor for steel, because it can be employed in neutral aqueous solutions [12,13], in solutions containing chloride ions [14,15], and in acidic media [11,16-19]. The mechanism of corrosion inhibition of steel by molybdate ion in neutral solution was first studied by Robertson in 1951 [20]. Later, Shams E1 Din and Wang [21] studied the corrosion of steel coupons

in an aerated l0 mM MoO_4^{2-} neutral aqueous solution at 30°C and they supported the passivation of steel. The stability of that passive film required the continuous presence of dissolved oxygen in solution to strengthen the passive film, while the presence of chloride ions promoted the corrosion of the steel. It has been reported that chloride ions are incorporated in the passive film during passive film formation in chloride-containing electrolyte [22]. More recently, Mu et al. [17] reported good inhibition efficiencies by molybdate on cold rolling steel in hydrochloric acid solution in the 0.1-0.5 M concentration range. These findings are indications of the potential of MoO_4^{2-} to be a good corrosion inhibitor for stainless steel in hydrochloric acid solution [11].

The speciation of molybdenum species in aqueous solutions depends on its concentration and the pH of the solution. The dominant species are MoO_4^{2-} in the pH range 7-12, protonated $Mo_7O_{24}^{6-}$ in the pH range 3-5, and $Mo_8O_{26}^{4-}$ below pH= 2 [19]. It has been reported that Mo(VI) exists as cationic polynuclear complexes in acid solution with solution pH extending from zero to 2 [23]. On the other hand, Cruywagen and coworkers [24], using potentiometric and NMR investigations, showed that the mononuclear species and the polyoxoanions $[Mo_7O_{24}]^{6-}$, $[HMo_7O_{24}]^{5-}$, $[H_2Mo_6O_{21}]^{4-}$ (at lower concentrations), $[H_3Mo_8O_{28}]^{5-}$, $[Mo_8O_{26}]^{4-}$, $[Mo_{18}O_{56}(H_2O)_8]^{4-}$ and some minor species (depending on conditions), give a satisfactory description of molybdenum(VI) equilibria at concentrations up to 1.0 M and pH down to 1 irrespective of the ionic medium. Therefore, several works support that the negative ions would predominate in solutions of very low pH, though the distribution diagram of molybdenum species in acidic solutions still generates some controversy in the literature [25].

In this paper, we report a study on the corrosion behaviour of 304 stainless steel in 0.5 M HCl and its inhibition by hexa-ammonium heptamolybdate at various concentrations. Weight loss, potentiodynamic polarization, and surface morphology characterizations were employed.

2. Experimental

2.1. Materials and sample preparation

An austenitic stainless steel AISI 304 supplied by Thyssen Krupp Materials International (Mülheim a.d. Ruhr, Germany) was considered. The composition of the metal was determined by Spark Emission Spectrometry as 18.2 wt.% Cr, 8.02 wt.% Ni, 1.91 wt.% Mn, 0.333 wt.% Si, 0.315 wt.% Mo, 0.304 wt.% Cu, 0.091 wt.% V, 0.057 wt.% N, ≤0.052 wt.% C, 0.037 wt.% Nb, 0.032 wt.% P, ≤0.01 wt.% S, 0.008 wt.% Ti, Fe in balance. Plates of size 1 cm x 1 cm x 0.1 cm have been used in this work. The plates were ground with emery papers of different grit size, thoroughly washed and ultrasonically cleaned in twice-distilled water and absolute ethanol, for 10 min, and finally dried in

air. All chemicals used in this work (namely hydrochloric acid, and hexa-ammonium heptamolybdate tetrahydrate) were reagent grade. 0.5 M hydrochloric acid aqueous solutions were prepared by dilution of the concentrated solution using twice-distilled water. Hexa-ammonium heptamolybdate tetrahydrate (AM, $((NH_4)_6Mo_7O_{24})\ 4H_2O$; chemical structure [26] shown in **Figure 1**) was added to the acid solution in concentrations ranging from 10^{-4} to 10^{-3} M. The pH value of the resulting solutions was 0.40 ± 0.02.

2.2. Weight loss measurements

Plates were immersed, in a hanging position, in 100 ml of 0.5 M HCl solutions containing different concentrations of the inhibitor. The specimens were weighed prior to immersion in 100 ml of 0.5 M HCl containing different concentrations of AM. These plates were totally immersed in the test electrolyte for 48 hours, using a glass hook to hold them vertically. Samples were retrieved from the test solution, carefully washed with high purity water in an ultrasound bath and subsequently dried in the oven, prior to weight loss measurements. The plates were reweighed up to 10^{-4} g for determining corrosion rate. The difference in weight of the steel plates was then taken as the weight loss. The weight loss tests were reproduced twice to guarantee the reproducibility of the results. The accuracy of the method was within 5%. All the tests were conducted in the naturally-aerated solutions at either 298 K or 308 K using a thermostat-cooling condenser for the temperature control. The samples were weighed before and after immersion, and weight losses were determined. The efficiency (S_W) of the corrosion inhibitor is defined as the relative reduction in weight loss of the metal substrate given by:

$$S_W = \frac{W_0 - W}{W} \times 100 \qquad (1)$$

where W_0 and W are the weight losses of stainless steel in the absence and in the presence of the inhibitor, respectively. Each measurement was performed on three separate stainless steel samples, and average values are given. The standard deviation of the observed weight loss was less than 6%. Additionally, the degree of surface coverage (θ) by the inhibitor was calculated using the following equation:

$$\theta = \frac{S_W}{100} \qquad (2)$$

2.3. Electrochemical measurements

The square stainless steel plates were connected as the working electrodes in stagnant 0.5 M

HCl aqueous solution at 298 K. Only one side of the specimen was in contact with the electrolyte (exposed area 1 cm^2). The remaining side was coated by a non-reactive and non-conductive varnish.

Electrochemical studies were performed using a thermostatted double jacket glass cell in the conventional three-electrode configuration. The potential of the working electrode was measured against the saturated calomel electrode (SCE, +0.240 V (SHE)). The SCE was connected through a KCl-containing agar-agar salt bridge, the tip of which was placed as close as possible to the surface of the working electrode in order to minimize the solution resistance between the test and reference electrodes. The counter electrode was a platinum plate of 6 cm^2. The electrical contact with the test electrode was made using a crocodile clip attached to a small strip of the steel plate. A volume of 100 ml of the naturally aerated electrolyte was introduced in the electrochemical cell.

Electrochemical measurements were performed using a potentiostat model Voltalab PRZ 100 (Radiometer-Analytical) under computer control. The corrosion behaviour of the SS was investigated in hydrochloric acid solution using potentiodynamic polarization techniques. The polarization resistance was measured by scanning the potential ±30 mV around their corrosion potential (E_{corr}) at a scan rate of 1 mV s^{-1}. The inhibition efficiencies for different concentrations of the inhibitors were calculated using the following equation:

$$S_P = \frac{R_p - R_{p0}}{R_p} \times 100 \quad (3)$$

where R_{p0} and R_p are the electrode polarization resistances determined in the absence and in the presence of a given concentration of the inhibitor, respectively.

The potentiodynamic polarization curves were recorded in the range extending from -1.0 to +0.8 V (SCE) in 0.5 M HCl aqueous solutions in the absence and in the presence of different inhibitor concentrations with a scan rate of 1 mV s^{-1}. The corrosion current density, j_{corr}, is related to the corrosion rate, and the inhibition efficiency was calculated with the following equation:

$$S_I = \frac{j_0 - j_{corr}}{j_0} \times 100 \quad (4)$$

where j_{corr} and j_0 are the corrosion current densities (expressed in mA cm^{-2}) determined in the presence and in the absence of the inhibitor, respectively**.** Additionally, the passivation current densities, j_{pass}, were determined from the potentiodynamic polarization curves by reading the current density values in the plateau following the corresponding active-passive transitions.

2.4. Morphological characterization

The surface of the 304 stainless steel samples was observed using an OLYMPUS BH2 UMA

microscope. The microscope provides magnifications up to 1000x.

3. Results

3.1. Weight loss measurements

Weight loss measurements were performed on plates immersed in 0.5 M HCl solution both in the presence and in the absence of the inhibitor up to 60 hours at room temperature. **Figure 2** shows that weight loss increases linearly with time (R^2 ~1) irrespective of the inhibitor concentrations, the slope of the lines decreased with the increase of the inhibitor concentration. The results obtained at different inhibitor concentrations are summarized in **Table 1**. Higher concentrations of the inhibitor led to a decrease in the values of the corrosion rate, while the inhibition efficiencies and the surface coverage increased. The increase of the inhibition efficiency and the associated decrease in the corrosion rate for growing concentrations of the inhibitor can be related to greater surface coverages by the inhibitor that affords corrosion protection to the stainless steel substrate. From the inspection of Fig. 2 and the data contained in Table 1 is readily concluded that the highest inhibitor efficiency of 91% was obtained when a $1x10^{-3}$ M concentration of heptamolybdate ion was added to 0.5 M HCl solution. Corrosion of the underlying stainless steel substrate still occurs due to incomplete coverage of the metallic surface by the inhibitor molecules, facilitating activation of the underlying metal and subsequent metal dissolution.

3.2. Open circuit potential determinations

The open-circuit potential (OCP) of the stainless steel electrodes in aerated 0.5 M HCl solution was found to stabilize around -0.48 V (SCE) in the inhibitor-free solution (see **Figure 3**). OCP values shifted to more noble potentials in the presence of the inhibitor, reaching a value of -0.12 V (SCE) when the inhibitor was present in $1x10^{-3}$ M concentration. From the inspection of the curves depicted in the inset of Fig. 3, variations in the time evolution of the OCP values determined in each solution could be found. The time needed to attain a steady state was about 3-4 minutes depending on the inhibitor concentration. Upon immersion in the electrolyte, the OCP values shifted to more negative potentials very rapidly, due to removal of the thin surface oxides formed in air, and it took only 2 to 5 seconds for the samples to attain an almost stationary value when immersed in the solutions (cf. inset in Fig. 3). Yet the OCP values continued shifting to more negative values for the next 30 min. A slightly different trend was observed in the solutions with the inhibitor concentrations $1x10^{-4}$ and $2x10^{-4}$ M because the shift of potential reversed to the positive direction after ca. 20 min. The achievement of a stationary value might be related to the invariability of the interface

composition. That is to say that the steel interface immersed in 0.5 HCl undergoes formation of oxides in addition to inhibitor adsorption and manifests a passivation phenomenon. It is observed that the OCP found for the sample immersed in the solution with the highest inhibitor concentration attains a stationary OCP value 0.36 V more positive than in the inhibitor-free solution.

3.3. Potentiodynamic polarization measurements

Figure 4 depicts the potentiodynamic polarization curves of 304 stainless steel in aerated stagnant 0.5 M HCl solutions both in the absence and in the presence of varying concentrations of hexa-ammonium heptamolybdate at 298 K. They were measured 30 min after the samples were immersed in the corresponding solution, thus allowing the samples to attain stationary OCP values. The curves were recorded in the potential range extending from -1.0 to +0.8 V (SCE). Active-passive transitions are found in all the cases, which are evidenced by a shoulder in the current-potential plots at potentials positive to their corresponding corrosion potential values. The potential range for the occurrence of the shoulder is similar in all the plots (namely between -0.3 and -0.2 V (SCE)), indicating the occurrence of a passivation process related to the formation of oxide layers on the surface of the samples. Conversely, the addition of AM to the hydrochloric acid solution produces a major shift in the E_{corr} to the positive direction, and this is accompanied by a reduction of both the anodic and the cathodic current densities.

Due to the occurrence of the active-passive transition on the anodic branch of the potentiodynamic polarization curves, the potential range for the linear Tafel behaviour is very short making it difficult to accurately determine the corresponding Tafel slope [27-29]. The curvature of the anodic branch may be attributed to the deposition of the corrosion products on the steel surface [29]. According to Amin and Ibrahim [30], and Bockris and Reddy [31], extrapolation of the cathodic branch would be sufficient to compute the corrosion current by Tafel extrapolation to corrosion potential. They argued that concentration effect due to passivation and dissolution may be the cause of the deviation from Tafel behaviour on the anodic branch. Thus, extrapolation of the cathodic Tafel region back to zero overvoltage would give the net rate of the cathodic reaction at the corrosion potential. This is also the net rate of the anodic reaction at the corrosion potential which verified by other non-electrochemical techniques [32]. Yet, other researchers have pointed out the limitation of the Tafel line extrapolation method in the determination of corrosion rates insofar that the latter is less accurate [28].

The values of the electrochemical parameters that can be extracted from the potentiodynamic polarization curves are collected in **Table 2**, and they are given as a function of the inhibitor concentration. Next, the inhibition efficiencies S_p, S_I, and the electrode polarization resistances, R_p,

were calculated for 304 stainless steel immersed in these solutions. The Tafel slopes of the cathodic reaction, β_c, vary slightly with the change in the concentration of the inhibitor. Conversely, the polarization resistance values and the inhibition efficiencies increased with the addition of different concentrations of AM. Furthermore, it is observed that the pitting potential E_p, the polarisation resistance R_p and the inhibition efficiencies S_P and S_I increase with higher concentrations of the inhibitor, whereas the opposite happens for the corrosion, j_{corr}, and the passivation, j_{pass}, current densities. An increase of pitting corrosion of passive 304 stainless steel by adding heptamolydate to pure water with small chloride contents (namely < 200 ppm) has already been reported [33], though the stability of the polyanion in this neutral environment might be rather low.

3.5. Morphological characterization

Optical microscopy was employed to examine the surface modification of the stainless steel samples that had been immersed in 0.5 M HCl solution, both with and without the corrosion inhibitor, for 1 hour. For the sake of comparison, the micrograph of an unexposed substrate is also given in **Figure 5**A. The micrograph of a blank stainless steel sample retrieved after immersion in 0.5 M HCl for one hour given in Fig. 5B shows evidence of a severe corrosive attack with the formation of several pits randomly distributed on the surface. Conversely, a sample retrieved after immersion in 0.5 M HCl containing $1x10^{-3}$ M AM exhibited less and smaller pits (cf. Fig. 5C). These findings support the ability of heptamolybdate ions to protect the steel and to retard its corrosion in HCl solutions. In addition, occurrence of corrosion product precipitation around the pits resulting from the aggressive attack to the stainless steel by chloride ions could be observed as well.

4. Discussion

The inhibition effects of heptamolybdate ions on the corrosion of 304 stainless steel in 0.5 M HCl solution at 25 ºC was characterized by weight loss and electrochemical methods. It is interesting to notice that, despite the difficulties experienced in the determination of the corrosion current j_{corr} from Tafel analysis, the values of the inhibition efficiencies determined from them, S_I, are close to those determined from the other methods, though they could be regarded less accurate. Increasing inhibitor concentration reduces the corrosion rate of the alloy. The results reveal that heptamolybdate ions are an efficient corrosion inhibitor even used in small concentration, effectively counteracting the low solubility of these species in the acid solution that hinders higher concentrations to be attained. On the other hand, it is worth pointing that the inhibitor efficiency obtained for the corrosion protection of 304 stainless steel in this work is ca. 5% higher than that previously reported

for cold rolling steel under similar experimental conditions [34].

Inhibition relies on the interaction of these species on the metal surface by reducing the metal dissolution process through the passive film. Increasing inhibitor concentration shifts the open circuit potential to more positive values, supporting that heptamolybdate ions mainly act as an anodic inhibitor. That is, the inhibitive effect is afforded by retarding the dissolution reaction of steel rather than modifying the kinetics of the cathodic hydrogen evolution reaction. Since potentiodynamic polarization results show the occurrence of an active/passive transition related to passivation, the inhibitor must participate in the formation of the protective film on the surface of 304 stainless steel that should avoid the direct contact of aggressive ions in the electrolyte with the surface of the metallic material. In other words, the formation of a surface film containing the inhibitor decreases the active surface area on the metal susceptible to localized corrosion. Indeed, a reduction of the passive current of almost two orders of magnitude resulted from the addition of $1x10^{-3}$ M AM to the test solution.

The corrosion inhibition efficiency of heptamolybdate ions can be greatly influenced by their adsorption on the stainless steel surface. It is considered that the primary step in the mechanism of corrosion inhibition in acid environments is the adsorption of the inhibitor on the metal surface [35,36], thus effectively competing with the adsorption of chloride ions [37,38]. In the case of moderate corrosion rates, and considering quasi-equilibrium adsorption, adsorption isotherms can provide valuable information on the interaction of the inhibitor ions with the metal surface. To reveal the adsorption behaviour of the inhibitor, the values of θ computed using equations (1), (3) and (4) were fitted to various isotherms, namely Langmuir, Frumkin and Temkin. Results showed that Langmuir isotherm led to the best fit on the basis of the correlation coefficient, R^2. Langmuir isotherm considers all adsorption sites to be equivalent and independent, the latter standing for the absence of interaction with neighboring sites whether occupied or empty. This isotherm is described by:

$$\frac{C}{\theta} = C + \frac{1}{K} \qquad (5)$$

where C is the concentration of the inhibitor, K is the equilibrium constant for the adsorption-desorption process, and θ is the surface coverage. **Figure 6** shows a linear relationship between C/θ and C with a very high correlation coefficient (R^2~1). The slope of the plot is close to unity, supporting Langmuirian adsorption for the process. This result agrees with a similar observation by Mu et al. in the case of cold rolling steel [17] from measurements taken at 25 ºC, though they reported that the system deviated greatly from the Langmuirian behaviour when the temperature was

raised to 35 ºC though only a very small change in the inhibitor efficiency was produced by this temperature change. In order to check this feature, a new set of measurements were conducted at 35 ºC using the weight loss method as before. The measured data are listed in **Table 3**, whereas the corresponding linear relationship between C/θ and C is also included in Figure 6. It is readily observable that good linearity, with slope close to 1, also occurs at the higher temperature. That is, the interaction of this ionic inhibitor with the stainless steel surface is satisfactorily described by the Langmuirian behaviour, conversely to the reports by Mu et al. [17]. It is interesting to notice that the environments investigated by Mu et al. maybe less acidic than those considered in our work. Though the same polyanions are actually formed from single MoO_4^{2-} ions when the pH becomes less than 6 according to [39,40]:

$$7\,MoO_4^{2-} + 8\,H^+ \quad \Leftrightarrow \quad Mo_7O_{24}^{6-} + 4\,H_2O \qquad (6)$$

protons are consumed and water molecules are formed, thus making the environment less aggressive for steel. In the current study such an effect was minimized by using AM as the chemical species to produce the electrolytic solutions.

Even more striking was the difference in the values of the thermodynamic parameters for inhibitor adsorption that are derived from our study compared to those reported in the literature. Large values of the adsorption equilibrium constant are now obtained, namely K = 5000 M^{-1}, thus revealing the high adsorption ability of the inhibitor on the surface of stainless steel. This equilibrium constant, K, is related to the standard adsorption free energy, $\Delta G°$, by:

$$K = \frac{1}{55.5}\exp\left(\frac{-\Delta G°}{RT}\right) \qquad (7)$$

where R and T are the universal gas constant and the absolute temperature, respectively. The computed value of the free energy of adsorption of heptamolydate ions on stainless steel was -31.1 kJ mol^{-1}, more than one order of magnitude greater than the values reported by Mu et al. for cold rolling steel [17]. The nature of the adsorptive process is often discussed in terms of the $\Delta G°$ values, and in many publications regarding corrosion inhibitors it is customary to establish that an absolute value of $|\Delta G°| < 20$ kJ mol^{-1} stands for a physisorption process, while $|\Delta G°| > 40$ kJ mol^{-1} would correspond to chemisorption [41-43]. Under such reasoning, the behavior of heptamolybdate would be possibly classified as a physisorption interaction, by considering that bond strength between the inhibitor ionic species and the surface is similar to that typically involved in van der Waals forces [44]. Indeed, the latter exhibit quite a wide range of values arising from differences in the geometry, size and electron density distribution in the adsorbing species even for a neutral species. By

accepting such an interpretation, chemical interaction between heptamolybdate ions and the metal surface would be discarded, as considered by Zhang et al. regarding the corrosion inhibition of AA6061 in NaCl solution by heptamolybdate ions [45]. But this feature is very unlikely for a charged ionic species such as heptamolybdate. Indeed, chemical interaction of molybdate ions with steel substrates is generally accepted in weakly acid and neutral solutions. An alternate approach may arise from considering that the geometry, size and charge density also greatly vary in the case of charged species when involving polyanions such as heptamolybdate. Indeed, heptamolybdate can even condense into a bigger ionic species $Mo_8O_{26}^{4-}$ at the pH values considered in this work [19], resulting in the formation of a more voluminous ion that presents smaller charge density. In this way, the charge density is smaller than for heptamolybdate, and certainly much smaller than for orthomolybdate anions, and adsorption should become more difficult due to its big volume. In that way, weaker inhibitor-metal interaction should be expected [46], but there is no need to rule out the eventual establishment of a chemical interaction between the inhibitor species and the metal surface. In fact, it has been proposed these polyanions present the ability to coordinate with an empty *d* orbital from iron to form a surface complex [47], and Fe^{3+} and Cr^{3+} were reported to form heteropoly anions such as $(Fe,Cr)Mo_6O_{24}^{9-}$ [48]. An alternate proposal considers the formation of molybdic acid (H_2MoO_4) and precipitation of salt films in these acidic environments, possibly containing chloride ions, which block pores and reactive corroding sites [1,13,49,50]. Additionally, orthomolybdate ions MoO_4^{2-} can be incorporated into passive films according to XPS observations [51,52]. For passive layers formed on near neutral NaCl solution [53], the anions were regarded to be added to the outer layer of the surface passive film without modification, thus forming $Fe_2(MoO_4)_3$, whereas the inner layer was composed by ferric oxi-hydroxides. A similar bilayer passivating oxide film, though involving the formation of polymeric molybdates, was proposed by Jakupi et al. to explain the inhibition of crevice corrosion on Alloy-22 specimens [54]. Local acidification within the occluded electrolyte volume inside a crevice, resulted in the precipitation of corrosion products with Raman signals consistent with the formation of polymolybdates according to equations (6) and (8):

$$8\,MoO_4^{2-} + 12\,H^+ \quad \Leftrightarrow \quad Mo_8O_{26}^{6-} + 6\,H_2O \qquad (8)$$

These Authors report that those species may have already existed as a polymeric gel during crevice corrosion, and they could observe them in solid form on the retrieved samples once dried [54]. Yet, we regard that there is no sufficient experimental evidence at this stage to discern the nature of the metal-inhibitor interaction formed between a big polyanion such as heptamolybdate and 304 stainless steel in 0.5 M HCl, and either inhibitor modelling or chemical analysis of the surface films would be

required to that end.

5. Conclusions

The ability of heptamolybdate ions to reduce the corrosion of 304 stainless steel in 0.5 M HCl solution was investigated at various concentrations of the inhibitor using weight loss and electrochemical determinations. The inhibition efficiencies determined using different methods were bigger for higher concentrations of the heptamolybdate ion, thus effectively enhancing the corrosion resistance of the stainless steel. Heptamolybdate ions can be regarded an efficient inhibitor for stainless steel in 0.5 M hydrochloric acid from the observation of inhibitor efficiency values above 90%.

Potentiodynamic polarization curves demonstrated that heptamolybdate ions acts as anodic inhibitor. The adsorption of the inhibitor onto the stainless steel surface follows Langmuir adsorption isotherm. The value of free energy of the adsorption was equal to -31.1 kJ mol^{-1}, indicating that there is an interaction between the heptamolybdate ion and the stainless steel surface.

Optical microscopy observations showed that there was a major reduction in both the number and the size of pits formed on stainless steel in 0.5 M HCl solutions when heptamolybdate inhibitor was present in the aggressive medium.

Acknowledgments

Financial support to this work by the CNRST through the competence Pôle PECCA (Rabat, Maroc), and by the Spanish Ministry of Economy and Competitiveness (MINECO, Madrid) and the European Regional Development Fund under grant CTQ2012-36787, are gratefully acknowledged.

References

1. A. Pardo, M.C, Merino, A.E. Coy, F. Viejo, R. Arrabal, E. Matykina, Effect of Mo and Mn additions on the corrosion behaviour of AISI 304 and 316 stainless steels in H_2SO_4, Corrosion Science 50 (2008) 780-794.
2. G.T. Burstein, C. Liu, R.M. Souto, S.P. Vines, Origins of pitting corrosion, Corrosion Engineering Science and Technology 39 (2004) 25–30.
3. M.G. Fontana, N.D. Greene, Corrosion Engineering, McGraw-Hill, New York, 1967, p. 51.

4. G.T. Burstein, P.C. Pistorius, S.P. Mattin, The nucleation and growth of corrosion pits on stainless steel, Corrosion Science 35 (1993) 57–62.
5. G.S. Frankel, N. Sridhar, Understanding localized corrosion, Materials Today 11(10) (2008) 38-44.
6. P.C. Pistorius, G.T. Burstein, Metastable pitting corrosion of stainless steel and the transition to stability, Philosophical Transactions of the Royal Society London A A341 (1992) 531-559.
7. G.T. Burstein, S.P. Mattin, Nucleation of corrosion pits on stainless steel, Philosophical Magazine Letters 66 (1992) 127-131.
8. N.S. Patel, S. Jauhariand, G.N. Meht, S.S. Al-Deyab, I. Warad, B. Hammouti, Mild steel corrosion inhibition by various plant extracts in 0.5 M sulphuric acid, International Journal of Electrochemical Science 8 (2013) 2635-2655.
9. M.H. Hussin, M.J. Kassim, Electrochemical studies of mild steel corrosion inhibition in aqueous solution by *Uncariagambir* extract, Journal of Physical Science 21 (2010) 1-13.
10. V.S. Saji, A review on recent patents in corrosion inhibitors, Recent Patents on Corrosion Science 2 (2010) 6-12.
11. G.O. Ilevbare, G.T. Burstein, The inhibition of pitting corrosion of stainless steels by chromate and molybdate ions, Corrosion Science 45 (2003) 1545–1569.
12. S. Ramesh, S. Rajeswari, Corrosion inhibition of mild steel in neutral aqueous solution by new triazole derivatives, Electrochimica Acta 49 (2004) 811–820.
13. M. Saremi, C. Dehghanian, M.M. Sabet, The effect of molybdate concentration and hydrodynamic effect on mild steel corrosion inhibition in simulated cooling water, Corrosion Science 48 (2006) 1404–1412.
14. N. Ebrahimi, M.H. Moayed, A. Davoodi, Critical pitting temperature dependence of 2205 duplex stainless steel on dichromate ion concentration in chloride medium, Corrosion Science 53 (2011) 1278–1287.
15. F. Eghbali, M.H. Moayed, A. Davoodi, N. Ebrahimi, Critical pitting temperature (CPT) assessment of 2205 duplex stainless steel in 0.1 M NaCl at various molybdate concentrations, Corrosion Science 53 (2011) 513–522.
16. S.A.M. Refaey, Inhibition of steel pitting corrosion in HCl by some inorganic anions, Applied Surface Science 240 (2005) 396–404.
17. G.N. Mu, X.H. Li, Q. Qu, J. Zhou, Molybdate and tungstate as corrosion inhibitors for cold rolling steel in hydrochloric acid solution, Corrosion Science 48 (2006) 445–459.
18. S.S. Abd El-Rehim, S.A.M. Refaey, F. Taha, M.B. Saleh, R.A. Ahmed, Corrosion inhibition of mild steel in acidic medium using 2-amino thiophenol and 2-cyanomethyl benzothiazole, Journal

of Applied Electrochemistry 31 (2001) 429-435.

19. J. Aveston, E.W. Anacker, J.S. Johnson, Hydrolysis of molybdenum(VI). Ultracentrifugation, acidity measurements, and Raman spectra of polymolybdates, Inorganic Chemistry 3 (1964) 735-746.
20. W.D. Robertson, Molybdate and tungstate as corrosion inhibitors and the mechanism of inhibition, Journal of the Electrochemical Society 98 (1951) 94-100.
21. A.M.S. E1 Din, L. Wang, Mechanism of corrosion inhibition by sodium molybdate, Desalination 107 (1996) 29-43.
22. M.A. Ameer, A.M. Fekry, F. El-Taib Heakal, Electrochemical behaviour of passive films on molybdenum-containing austenitic stainless steels in aqueous solutions, Electrochimica Acta 50 (2004) 43–49.
23. Z. Li, Y.C. Chu, A literature review of the recovery of molybdenum and vanadium from spent hydrodesulphurization catalysts: Part II: Separation and purification, Hydrometallurgy 98 (2009) 10-20.
24. J.J. Cruywagen, A.G. Draaijer, J.B.B. Heyns, E.A. Rohwer, Molybdenum(VI) equilibria in different ionic media. Formation constants and thermodynamic quantities, Inorganica Chimica Acta 331 (2002) 322–329.
25. M. Lee, S. Sohn, M. Lee, Ionic equilibria and ion exchange of molybdenum(VI) from strong acid solution, Bulletin of the Korean Chemical Society 32 (2011) 3687-3691.
26. L.X. Song, M. Wang, Z. Dang, F.Y. Du, Meaningful differences in spectral performance, thermal behavior, and heterogeneous catalysis between ammonium molybdate tetrahydrate and its adduct of β-cyclodextrin, Journal of Physical Chemistry B 114 (2010) 3404–3410.
27. N.T. Thomas, K. Nobe, Electrochemical behavior of titanium - Effect of Ti(III) and Ti(IV), Journal of the Electrochemical Society 119 (1972) 1450-1456.
28. G. Quartarone, T. Bellomi, A. Zingales, Inhibition of copper corrosion by isatin in aerated 0.5 M H_2SO_4, Corrosion Science 45 (2003) 715–733.
29. M.A. Amin, S.S. Abd El-Rehim, E.E.F. El-Sherbini, O.A. Hazzazi, M.N. Abbas, Polyacrylic acid as a corrosion inhibitor for aluminium in weakly alkaline solutions. Part I: Weight loss, polarization, impedance, EFM and EDX studies, Corrosion Science 51 (2009) 658–667.
30. M.A. Amin, M.M. Ibrahim, Corrosion and corrosion control of mild steel in concentrated H_2SO_4 solutions by a newly synthesized glycine derivative, Corrosion Science 53 (2011) 873–885.
31. J.O'M. Bockris, A.K.N. Reddy, Modern Electrochemistry, vol. 2, Plenum Press, New York, 1972, p. 1265.
32. E. McCafferty, Validation of corrosion rates measured by the Tafel extrapolation method,

Corrosion Science 47 (2005) 3202-3215.

33. C.R. Alentejano, I.V. Aoki, Localized corrosion of 304 stainless steel in pure water by oxyanions tungstate and molybdate, Electrochimica Acta 49 (2004) 2779-2785.
34. A. El Ouafi, Y. Abed, B. Hammouti, S Kertit, Effect of acidity level $R_o(H)$ on the corrosion of steel in concentrated HCl solutions, Annales de Chimie Science des Matériaux 26-5 (2001) 79-84.
35. I.L. Rozenfeld, Corrosion Inhibitors, Mc-Graw Hill, New York, 1981, p. 97.
36. J.G.M. Thomas, The mechanism of corrosion prevention by inhibitors, in: L.L. Shrier, R.A. Jarman, G.T. Burstein (Eds.), Corrosion, Third edition, Butterworth-Heinemann, Oxford, 1994, pp. 17:40-17:65.
37. G. Ruijini, M. B. Ives, The influence of addition of molybdate ions on pit growth in UNS S30100 stainless steel in chloride solution, Corrosion 45 (1989) 572-574.
38. H.H. Uhlig, J.R. Gilman, Pitting of 18-8 stainless steel in ferric chloride inhibited by nitrates, Corrosion 20 (1964) 289t-293t.
39. H. Yashiro, A. Oyama, K. Tanno, Effects of temperature and potential on the inhibitive action of oxoacid salts for pitting in high-temperature chloride solutions, Corrosion 53 (1997) 290-297.
40. M. Ürgen, A.F. Çakir, The effect of molybdate ions on the temperature dependent pitting potential of austenitic stainless steels in neutral chloride solutions, Corrosion Science 32 (1991) 835-852.
41. V. Branzoi, F. Branzoi, M. Baibarac, The inhibition of the corrosion of Armco iron in HCl solutions in the presence of surfactants of the type of N-alkyl quaternary ammonium salts, Materials Chemistry and Physics 65 (2000) 288-297.
42. X. Li, S. Deng, H. Fu, Triazolyl blue tetrazolium bromide as a novel corrosion inhibitor for steel in HCl and H_2SO_4 solutions, Corrosion Science 53 (2011) 302-309.
43. H. Zarrok, A. Zarrouk, B. Hammouti, R. Salghi, C. Jama, F. Bentiss, Corrosion control of carbon steel in phosphoric acid by purpald – Weight loss, electrochemical and XPS studies, Corrosion Science 64 (2012) 243-252.
44. P. Atkins, J. de Paula, Atkins' Physical Chemistry, Seventh edition, Oxford University Press, Oxford, 2002, p. 988.
45. D.Q. Zhang, X. Jin, B. Xie, H.G.. Joo, L.X. Gao, K.Y. Lee, Corrosion inhibition of ammonium molybdate for AA6061 alloy in NaCl solution and its synergistic effect with calcium gluconate, Surface and Interface Analysis 44 (2012) 78-83.
46. M.A. Stranick, The corrosion inhibition of metals by molybdate. Part I. Mild steel, Corrosion 40 (1984) 296-302.

47. P.W. Shen, Y.X. Che, Y.J. Luo, Y.D. Gu, G.Y. Xie, Y. Song, S.L. Jin, Texbook of Inorganic Chemistry, vol. 8, Science Presss, Beijing, 1998, p. 472.
48. W.J. Tobler, S. Virtanen, Effect of Mo species on metastable pitting of Fe18Cr alloys - A current transient analysis, Corrosion Science 48 (2006) 1585-1607.
49. M.A. Cavanaugh, J.A. Kargol, J. Nickerson, N.F. Fiore, Anodic dissolution of a Ni-based superalloy, Corrosion 39 (1983) 144-150.
50. M. Rincón Ortíz, M.A. Rodríguez, R.M. Carranza, R.B. Rebak, Oxyanions as inhibitors of chloride-induced crevice corrosion of Alloy 22, Corrosion Science 68 (2013) 72-83.
51. A.A. El Hosary, M.M. Badran, R.M. Saleh, H.A. El Dahan, Corrosion inhibition of 304 stainless steel in H_3PO_4-Cl^- solutions by chromium, molybdenum, nitrogen, tungsten, and boron anions. Part 2: Auger electron spectroscopy measurements, British Corrosion Journal 25 (1990) 197-201.
52. H.A. El Dahan, Pitting corrosion inhibition of 316 stainless steel in phosphoric acid-chloride solutions. Part I. Potentiodynamic and potentiostatic polarization studies, Journal of Materials Science 34 (1999) 851-857.
53. A.A. Al-Refaie, J. Walton, R.A. Cottis, R. Lindsay, Photoelectron spectroscopy study of the inhibition of mild steel corrosion by molybdate and nitrite anions, Corrosion Science 52 (2010) 422-428.
54. P. Jakupi, F. Wang, J.J. Noël, D.W. Shoesmith, Corrosion product analysis on crevice corroded Alloy-22 specimens, Corrosion Science 53 (2011) 1670-1679.

Table 1.

Corrosion parameters obtained from weight loss of 304 stainless steel in 0.5 M HCl containing different concentrations of AM at 298 K.

C, M	*W*, mg cm^{-2} day^{-1}	Correlation coefficient (R^2)	S_W, %	θ
0	8.16	0.998	---	---
$1x10^{-4}$	5.33	0.992	34.7	0.347
$2x10^{-4}$	3.77	0.994	53.8	0.538
$5x10^{-4}$	2.04	0.990	75.0	0.750
$8x10^{-4}$	1.24	0.990	85.0	0.850
$1x10^{-3}$	0.72	0.990	91.2	0.910

Table 2.

Corrosion parameters obtained from potentiodynamic polarization curves of 304 stainless steel in 0.5 M HCl containing different concentrations of AM at 298 K.

C, M	E_{corr}, V (SCE)	E_p, V (SCE)	j_{corr}, µA cm^{-2}	j_{pass}, µA cm^{-2}	$-\beta_c$, mV dec^{-1}	R_p, Ω cm^2	S_P, %	S_I, %
0	-0.480	+0.030	587	1610	151	50.7	--	---
$1x10^{-4}$	-0.437	+0.033	358	802	146	79.3	36.1	39.0
$2x10^{-4}$	-0.424	+0.047	307	562	147	90.8	44.8	47.7
$5x10^{-4}$	-0.402	+0.061	240	269	135	155.2	67.3	59.4
$8x10^{-4}$	-0.380	+0.174	126	191	133	286.2	82.3	78.5
$1x10^{-3}$	-0.278	+0.222	68	46	132	450.2	88.7	88.4

Table 3.

Corrosion parameters obtained from weight loss of 304 stainless steel in 0.5 M HCl containing different concentrations of AM at 308 K.

C, M	*W*, mg cm^{-2} day^{-1}	S_W, %	θ
0	20.42	---	---
$1x10^{-4}$	13.80	32.4	0.32
$2x10^{-4}$	10.92	46.5	0.46
$5x10^{-4}$	8.76	57.1	0.57
$8x10^{-4}$	7.40	64.4	0.64
$1x10^{-3}$	5.40	73.6	0.73

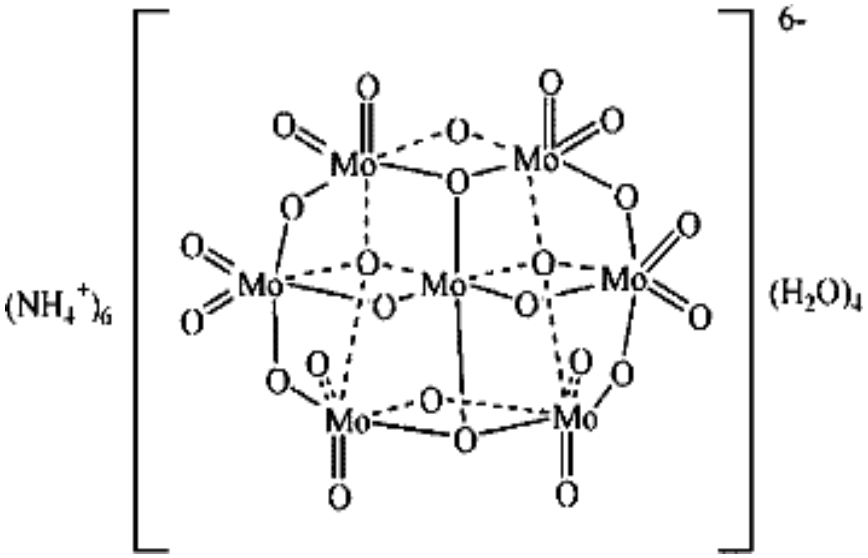

Figure 1. Chemical structure of hexa-ammonium heptamolybdate tetrahydrated (AM) according to ref. [26].

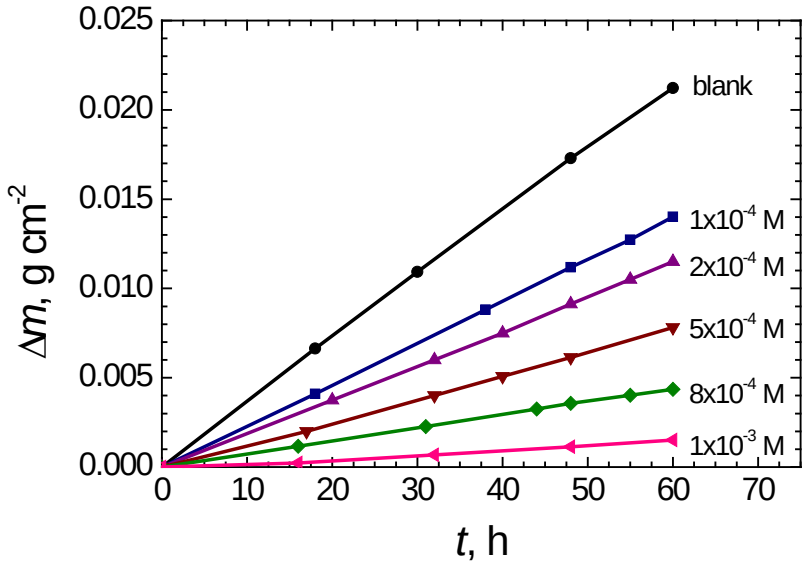

Figure 2. Time evolution of the weight loss experienced by 304 stainless steel samples in 0.5 M HCl in containing different concentrations of AM at 298 K.

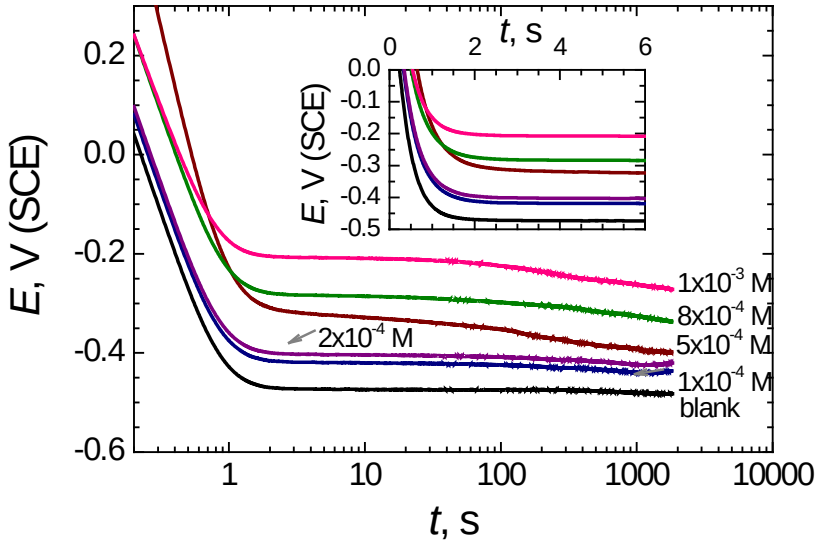

Figure 3. Time evolution of the open circuit potential values experienced by 304 stainless steel in 0.5 M HCl containing different concentrations of AM at 298 K.

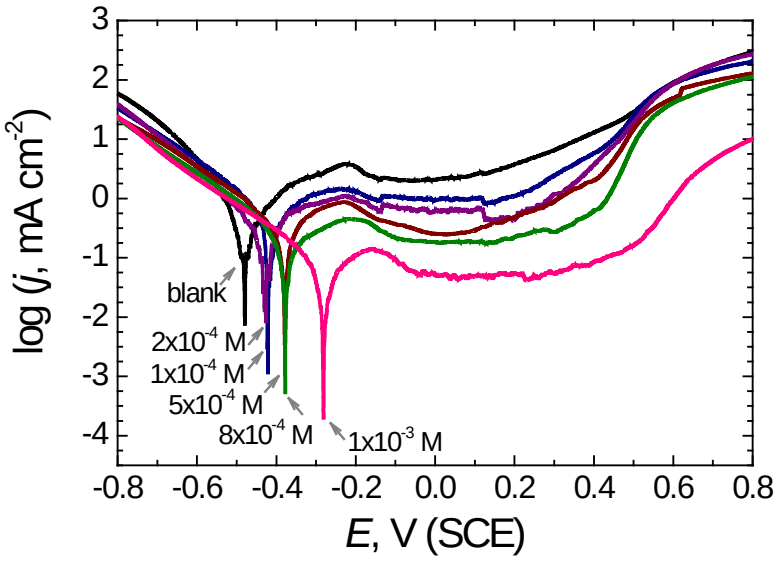

Figure 4. Potentiodynamic polarization curves of 304 stainless steel in 0.5 M HCl containing different concentrations of AM at 298 K. Scan rate: 1 mV s^{-1}.

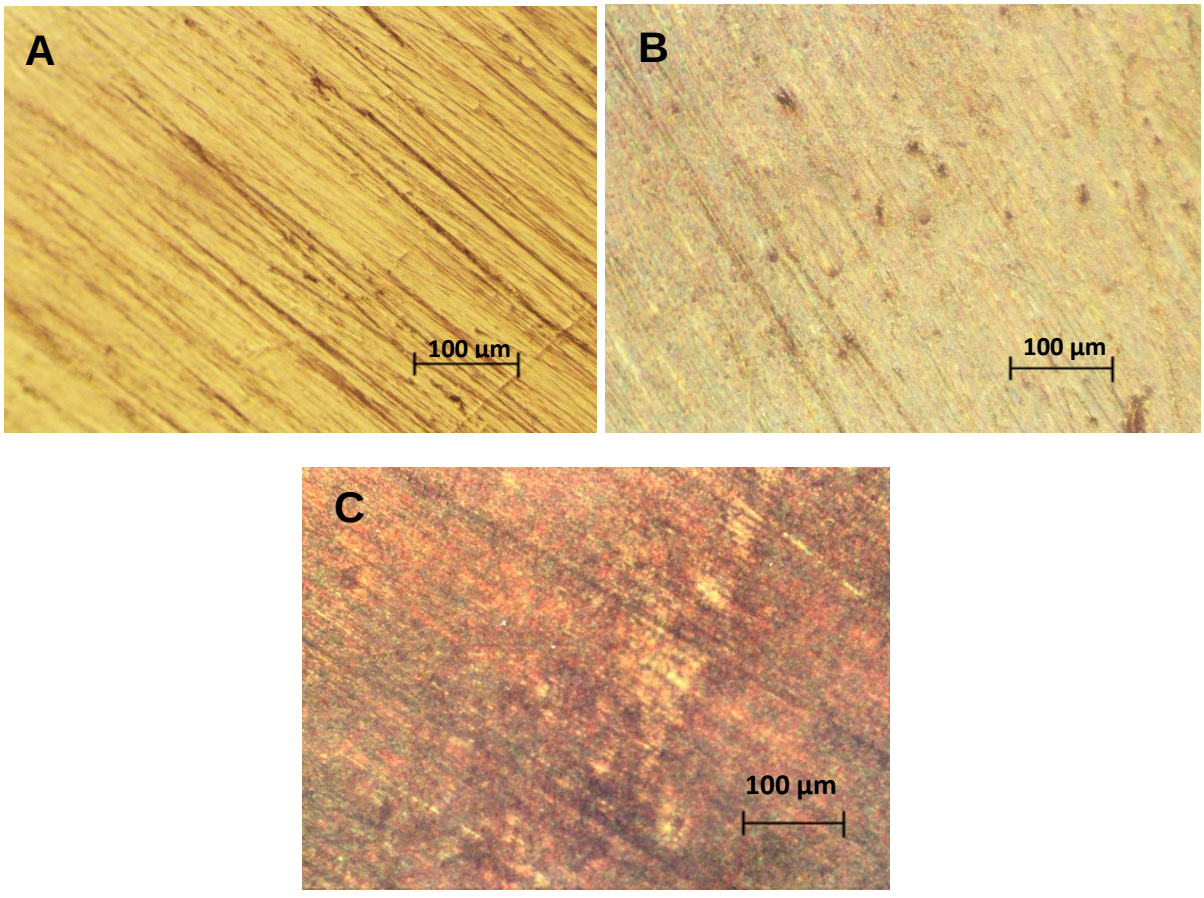

Figure 5. Optical micrographs of: (A) 304 stainless steel before exposure to 0.5 M HCl (blank), (B) 304 stainless steel sample exposed to 0.5 M HCl for 1 h, and (C) 304 stainless steel sample exposed to 0.5 M HCl + $1x10^{-3}$ M AM for 1 h.

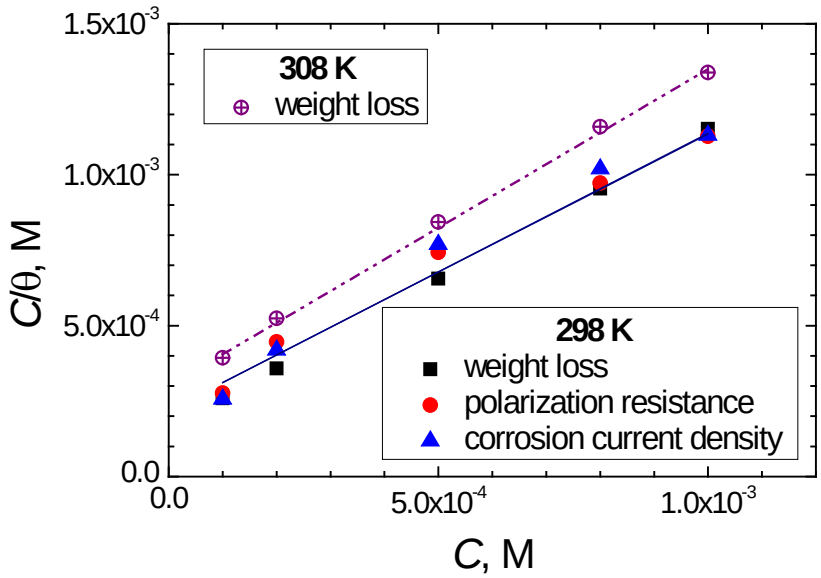

Figure 6. Langmuir adsorption plots of 304 stainless steel in 0.5 M HCl solution containing different concentrations of AM. At 298 K, the plots were determined from weight loss, polarization resistance and corrosion current density data determined using equations (1), (3) and (4); and at 308 K, the plot was determined from weight loss data.